Indian J Phys. 79 (3), 239-243 (2005)

AN INTERNATIONAL JOURNAL
IJP

Compton scattering study of samarium

B L Ahuja*, H Malhotra and M Sharma
Department of Physics, College of Science Campus,
M L Sukhadia University, Udaipur-313 001, Rajasthan, India
E-mail blahuja@yahoo.com

Received 14 July 2004, accepted 20 January 2005

Abstract : The isotropic Compton profile of samarium is presented in this work. The measurement has been made using our 661.65 keV 20 Ci ^{137}Cs Compton spectrometer. The results are compared with our calculations based on renormalised-free-atom (RFA) and free electron models. It is seen that the RFA calculation for configuration $4f^{6}5d^{0}6s^{2}$ (with e^{-}-e^{-} correlation) is in better agreement with the experiment. Using our RFA model, we have also derived the cohesive energy of samarium. A comparison of RFA based cohesive energy with the available band structure data shows the applicability of the RFA model in calculating the electronic structure of rare-earth elements.

Keywords Compton profile, electron momentum density, electron-electron correlation effects, cohesive energy, rare-earths

PACS Nos. 71.15.Nc, 71.20.Eh, 31.25.Qm, 78.70.Ck

1. Introduction

Samarium (Sm) belongs to the lanthanides group with rhombohedral structure. It has been found to produce materials with highly desirable magnetic properties. Considerable works, which mainly include energy position of $4f$ levels [1-3], valence states and their stability [4-7] and cohesive properties [8-11] have been reported on Sm along with other rare-earth elements.

It is well established that the Compton scattering, which is inelastic scattering of X-rays, can be utilized to probe the ground-state electronic properties of materials [12]. If the direction of the scattering vector $\boldsymbol{k}$ is chosen to be along the z-axis and the integration of electron momentum density $\rho(\boldsymbol{p})$ is over a constant plane, then the Compton profile is given by

$$J(p_z) = \iint \rho(\boldsymbol{p}) dp_x dp_y \,. \qquad (1)$$

The Compton profile experiments are extremely useful due to two reasons: (a) these connect the measured scattering cross section directly to the electronic ground state wave functions. Therefore, such measurements offer a straight forward way to check the applicability of band structure calculations for different materials (b) the contribution of the valence electrons is located close to the peak of the Compton profile and could therefore, easily be separated from the broad contribution of the core electrons.

There are some advantages if photons with high incident energies can be used to probe the electronic structure of heavy materials. This is particularly true in case of rare earth elements in which the binding energy of the K-shell electrons are of the order of 50 keV and therefore, can not be treated within the impulse approximation [12], when a low incident energy (like 60 keV from ^{241}Am) is used. Earlier, the Compton profile of Sm has been measured by Varghese *et al* [13] using 300 mCi ^{241}Am source and a co-axial Ge detector. The data has been compared only with the free atom Compton profile. An inspection of the data [13] suggests that it may have serious problems due to :

(i) Relatively poor resolution :

Instead of using a planar HPGe detector that gives a reasonably good resolution (530 eV at 122 keV; Gaussian FWHM), the authors have used co-axial Ge detector (resolution 780 eV at 122 keV). In a.u. units of momentum scale (where $e = m = \hbar = 1$ and $c = 137.036$) this resolution (say about 0.8 a.u.) is relatively poor and is insufficient to draw any conclusion from the data.

* Corresponding Author

(ii) Overlapping of fluorescent X-rays of Sm in Compton region :

Besides failure of impulse approximation in the measurements, the K-fluorescent lines (energy range 40 keV to 47 keV) emitted during the Compton measurements on Sm are expected to be in the Compton profile region (44 keV to 52 keV). Therefore, the fluorescence lines might have overlapped in the Compton region making these measurements as meaningless.

To continue our systematic study of Compton profiles of rare-earth elements [14], in this paper we present an accurate isotropic Compton profile of Sm using our ^{137}Cs Compton spectrometer. Due to practical difficulties (like chemical reactivity and requirement of ultra high vacuum conditions) in growing the required size (about 15 mm dia and 3 mm thickness) of single crystals of Sm, we have decided to measure the isotropic momentum density of Sm. To compare our experimental data, in absence of band structure calculations, we have employed renormalized-free atom (RFA) and free-electron models. The RFA profiles are also corrected for $e^- - e^-$ correlation effect. To check, the applicability of RFA model in the case of rare earths, we have also derived cohesive energy of Sm and compared it with available experimental and theoretical data.

2. Experiment

Compton profile of Sm has been measured using a 20 Ci ^{137}Cs Compton spectrometer [15]. The basics of the experimental set-up are shown in Figure 1. The performance of the spectrometer was tested using standard samples like Al and Ta. Gamma-rays of 661.65 keV were scattered through a mean angle of 160° ± 0.6° from a powder sample. The high purity (more than 99.9%) powder sample (bulk density-1.88 gm/cm^3) was kept in an ampoule having bulk thickness of 3 mm and mylar windows.

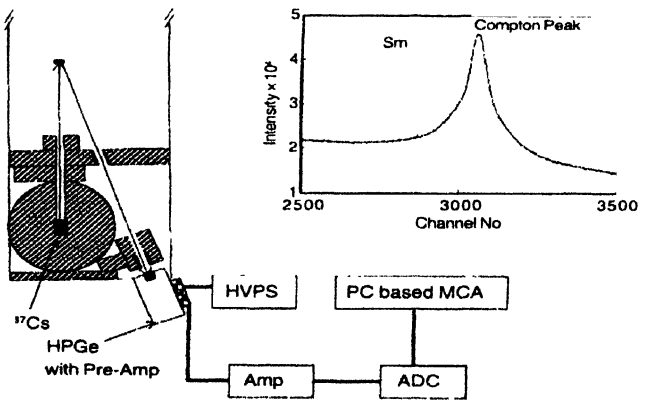

Figure 1. Layout of 20 Ci ^{137}Cs Compton spectrometer and associated electronics. ^{137}Cs source is located in a large lead block (22 cm diameter x 22 cm height) with a rotatable beam shutter. The lined area indicates extensive lead shielding. About 2000 Kg lead has been used for biological shielding and fabrication of different components of the spectrometer. In the inset, the raw Compton profile data for Sm is shown.

The spectrum of the scattered radiations was recorded with a Ge solid-state detector (Model GL0210P) and associated electronics (Canberra, USA made) like Spectroscopy Amplifier (Model 2022), Analog to Digital Converter (ADC Model 8701), Multi Channel Analyser (Accuspec B). Further, Genie 2000 MCA software was used to transfer the data in the CPU of our personal computer. The overall momentum resolution of the spectrometer that involves detector resolution and geometrical divergence was 0.40 a.u. (Gaussian FWHM). The resolution of our set-up is much better than any ^{241}Am Compton spectrometer with HPGe detector (0.60 a.u.). The data were accumulated for about 240 hours which resulted about 46,000 counts at the Compton peak (channel width 0.035 a.u.) and over 17 million integrated counts in the Compton region (–7 to + 7 a.u.). During the measurement, the stability of the system was checked from time to time using weak ^{57}Co and ^{133}Ba calibration sources.

After the background correction, the data were processed by application of a series of energy-dependent corrections like instrumental resolution (partial), detector efficiency, sample absorption, Compton cross-section *etc.* using a well-tested scheme of Warwick group [16]. The correction for instrumental resolution was restricted to stripping the low energy tail off the resolution function and smoothing the data [16], leaving the theory to be convoluted with the Gaussian of 0.40 a.u. (FWHM). A Monte Carlo procedure [17] was employed to determine the energy distribution of the multiple scattering. The contribution from the multiple scattering (in the momentum range 0 to +10 a.u.) was found to be 5.1%. After application of data processing routines, the high-energy side of the profile was normalized to the free atom value of 23.70 electrons over the momentum range 0 to 7 a.u. [18].

3. Calculations

(a) RFA calculation :

Since theoretical Compton profiles from band structure calculations for Sm are not available, we have computed the Compton profile using RFA model [19, 20]. In our earlier Compton scattering investigation on light metals, 3*d*, 4*d* and a few 5*d* transition metals, this model has been applied successfully [see, for example, Refs. 20-26]. The formulae for computing the Compton profiles of valence electron within the RFA scheme are available in print [19, 20]; here, we give only the computational details.

In the present calculation, approximate wave function for the crystal is derived by truncating the atomic wave function [27] at Wigner-Seitz (WS) radius and by renormalizing them to one per electron within the WS sphere to preserve the charge neutrality. It turned out that in Sm, only 68 % of the atomic 6*s* electron wave function was inside the WS sphere, while for 4*f* electrons, this number was nearly 100 %. Figure 2 shows the

shape of 6*s* wave functions for Sm, before and after renormalisation. To incorporate the crystalline effects, the contribution of 25 shortest reciprocal lattice vectors was considered. It is worthwhile to mention here that the isotropic Compton profile is almost independent of the structure of the sample, the determining factor being the average electron density, as mentioned by Ahuja *et al* [20, 24], Bacalis *et al* [28] and Papanicolaou *et al* [29]. In our RFA calculations, we have assumed the rhmobohedral (RHL) structure of Sm as a simple cubic, while computing the reciprocal lattice vectors involved in the RFA scheme.

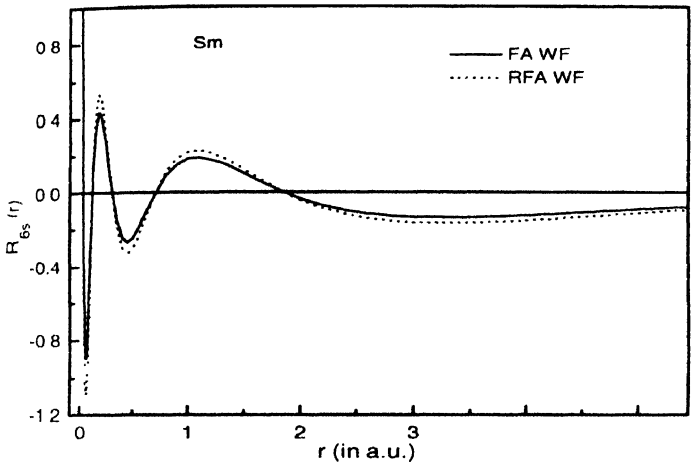

Figure 2. The free atom (FA) and renormalized-free-atom (RFA) wave functions (WFs) inside the Wigner-Seitz sphere of Sm. The FA wave function for 6s electrons are taken from the tables of Fischer [27].

(b) Free electron calculation:

In case of an isotropic momentum distribution, eq. (1) reduces to the well-known form:

$$J(p_z) = 2\pi \int_{p_z}^{\infty} dp\, \rho(p) p \,. \tag{2}$$

If we consider the valence electrons in a metal as a non-interacting electron gas, then the momentum density is given by

$$\rho(p) = \text{constant} = \frac{n}{\frac{4}{3}\pi p_F^3} \quad \text{for } p \le p_F \tag{3}$$

where n is the number of free electrons per site and p_F is the Fermi momentum.

Substitution of $\rho(p)$ from eq. (3) to eq. (2) gives

$$J(p_z) = \frac{3n}{4p_F^3}\left(p_F^2 - p_z^2\right) \quad \text{for } p_z \le p_F \,. \tag{4}$$

The free electron Compton profile is then an inverted parabola including discontinuities of the first derivative at $\pm p_F$. Using eq. (4), we have also calculated the free electron Compton profile for 6*s* electrons of Sm.

To get a total profile in the momentum range 0 to +7 a.u., the Compton profiles for core and 4*f* electrons were directly taken from the tables of Biggs *et al* [18].

4. Results and discussion

In Table 1, we have listed the experimental Compton profile of Sm together with the unconvoluted RFA for [Xe] $4f^6 5d^0 6s^2$ and $4f^7 5d^0 6s^1$ configurations and the free-electron profile. In the case of our RFA calculation for configuration $4f^6 5d^0 6s^2$, we have also incorporated the $e^- - e$ correlation correction following the prescription of Das and Chaddah [30], which was found to be very successful in case of Mg metal [31]. It is worth mentioning here that the electron correlation moves some of the momentum density from below to above the Fermi momentum.

Table 1. Experimental isotropic Compton profile of Sm. Also included here are the (unconvoluted) RFA Compton profiles (with and without $e^- - e^-$ correlation correction) and free electron (FE) Compton profiles. Experimental errors ($\pm\sigma$) at few points are also shown. All quantities are in a.u. For a reliable comparison with the experiment, the theoretical values have to be convoluted with the resolution of the experiment.

pz	J(pz)				
	Free electron	RFA ($4f^6 5d^0 6s^2$)	RFA ($4f^6 5d^0 6s^2$) with $e^- - e$ corr.	RFA ($4f^7 5d^0 6s^1$)	Experiment
0 00	11.47	10 21	10 18	9.47	9.26± 0.025
0 10	11 28	10 07	10 04	9 33	9.20
0 20	10 67	9 76	9 73	9 02	9 05
0 30	9 72	9 14	9 14	8 39	8 81
0 40	8 38	8 51	8 55	8 03	8.60
0 50	7.52	7.97	8.00	7.80	8.34
0 60	7 26	7 71	7 71	7 54	8 20
0.70	6 97	7 39	7.39	7 22	7 65
0.80	6.64	7 04	7 04	6 88	7 23
1.00	5.98	6 30	6 30	6.15	6 37± 0 019
1 20	5.39	5.59	5.59	5.49	5 73
1 40	4.90	5.00	5.00	4 97	5.10
1.60	4.53	4 56	4.56	4.59	4 68
1.80	4.24	4 25	4 25	4 30	4.32
2 00	4.01	4.02	4 02	4.07	3 95± 0 014
3.00	3.07	3 07	3.07	3 10	3.03± 0.011
4.00	2.21	2.21	2.21	2.23	2.21± 0.008
5.00	1.60	1.60	1.60	1.61	1.63± 0.007
6.00	1.23	1.23	1.23	1.24	1.27± 0.005
7.00	1 00	1.00	1.00	1 01	1.01± 0.004

Figure 3 shows the difference profiles (ΔJ) between convoluted theory and our experiment.

It can be seen from this figure that the convoluted free electron model profile gives a very poor agreement with the experiment, which may be due to its unrealistic assumption. The convoluted RFA profile for configuration $4f^{6}5d^{0}6s^{2}$ with e -e correlation gives a good overall fit with the experiment. It is also verified separately by χ^2 fitting for different combinations of theoretical values (with and without e^-–e^- correlation correction). To show the overall shape of total profiles, in the inset of Figure 3, we have plotted the experimental $J(p_z)$ and the best fit calculated curve (convoluted RFA $4f^{6}5d^{0}6s^{2}$ with e-e correlation). From Figure 3 and its inset, it is seen that in the low momentum region, the best-fit RFA profile (with e^-–e^- correlation) is higher than the experiment. This may be due to *spd-f* hybridization in the solid state phase of the Sm. We believe that the Compton profile corresponding to 6*p* or 5*d* electrons of the Sm is expected to be flatter than the 6*s* electrons.

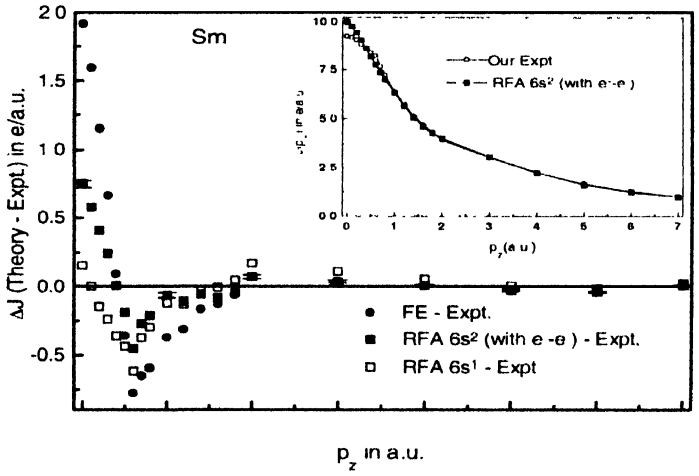

Figure 3. A plot of difference between experiment and convoluted RFA model for $4f^{6}5d^{0}6s^{2}$ (with e –e correlation) and $4f^{7}5d^{0}6s^{1}$ configurations. Difference between convoluted free electron profile (FE) and the experiment is also shown. The absolute experimental profile and the best-agreed convoluted RFA profile for configuration $4f^{6}5d^{0}6s^{2}$ (with correlation correction) are shown in the inset. The statistical errors (2σ band) are shown for a few points.

Hence, incorporation of the contribution of 6*p* or 5*d* electrons in the theoretical Compton profile calculations will reduce the magnitude of the total theoretical profile in the low momentum region. Then, it will lead to a better agreement between theory and experiment. Unfortunately, 6*p* or 5*d* electron wave functions or Compton profiles are not available in the literature, therefore it is not possible to consider in detail, the presence of 6*p* and 5*d* electrons in the valence band of Sm in its bulk state. The overall picture obtained is consistent with the previous theoretical work on Fermi surfaces [32] and LMTO calculations of Lundin *et al* [3] where a better agreement between theory and experiment is obtained when one considers the 4*f* state as valence electrons even though part of these 4*f* states are treated as occupied core state. This is also supported by the first principles electronic structure calculations of Strange *et al* [6], who had split 4*f* band into two sub-bands and concluded that the *f* band hybridizes with the *s* – *d* bands that straddles the Fermi energy.

The cohesive energy E_{coh} is defined as the difference between the total ground-state energy of the solid state and the energy of the individual isolated atoms. The cohesive energy from the Compton profile data [33] is given as

$$E_{coh} = \int_{0}^{p_{max}} p^2 \left[J_s - J_{fa} \right] dp ,$$

where J with subscript *s* and *fa* refer to solid and free atom profiles, respectively. The values of J_s were taken from the present RFA calculations and those for J_{fa} from the free atom tables [18]. As reported by Holt and Cooper [33] and Mittal *et al* [23], the calculation of cohesive energy from the experimental Compton profile is a difficult task due to weighting of p^2 in the high momentum region. Therefore, we have used the RFA profiles for the calculation of cohesive energy.

Table 2. RFA based cohesive energy (E_{coh}) for samarium. Also included here are the results of other investigators.

Cohesive energy (in eV)					
RFA		LMTO [10]		Interpolation technique [9]	Experiment [34]
$4f^{6}5d^{0}6s^{2}$	$4f^{7}5d^{0}6s^{1}$	LDA	GGA		
5.33	5.78	4.49	5.10	4.63	2.10

In Table 2, our RFA based E_{coh} is compared with the cohesive energy calculations using local density approximation (LDA) and generalized gradient approximation (GGA) within the full potential LMTO [10]. Also included here are the cohesive energy values from interpolation technique [9] and the experimental data [34]. Our calculated E_{coh} for the best agreed RFA $4f^{6}5d^{0}6s^{2}$ configuration shows a good agreement with LMTO-GGA calculations [10], although our value is higher.

5. Conclusions

In this work, it has been shown that the RFA model for configuration $4f^{6}5d^{0}6s^{2}$ with e^- – e^- correlation, despite the difference in the low momentum region, gives a better agreement with our experimental data. Our measurement indicates the presence of 5*d* and 6*p* electrons in solid phase of Sm. The RFA ($4f^{6}5d^{0}6s^{2}$)-based cohesive energy of Sm is in good agreement with the LMTO-GGA calculations. To conclude, relativistic band structure based Compton profile calculations are needed to describe all the features highlighted in our experiment.

Acknowledgment

This work is partially supported by a grant from Department of Science and Technology (DST), New Delhi vide grant No. SP/S-2/M03/99.

References

[1] B Johansson and A Rosengren *Phys. Rev.* **B14** 361 (1976)

[2] B Johansson *Phys. Rev.* **B20** 1315 (1979)

[3] U Lundin, I Sandalov, O Eriksson and B Johansson *Solid State Commun.* **115** 7 (2000)

[4] B Johansson *Phys. Rev.* **B19** 6615 (1979)

[5] A Delin, L Fast, B Johansson, J M Wills and O Eriksson *Phys. Rev. Lett* **79** 4637 (1997)

[6] P Strange, A Svane, W M Temmerman, Z Szotek and H Winter *Nature* **399** 756 (1999)

[7] L Petit, A Svane, Z Szotek, P Strange, H Winter and W M Temmerman *J. Phys.. Condens. Matter* **13** 8697 (2001)

[8] B Johansson and P Munck *J Less-Common Met* **100** 49 (1984)

[9] M S S Brooks and B Johansson *J Phys* **F13** 197 (1983), Also B Johansson and A Rosengren *Phys Rev* **B14** 1367 (1975)

[10] A Delin, L Fast, B Johansson, O Eriksson and J M Wills *Phys Rev* **B58** 4345 (1998)

[11] A Delin, L Fast, O Eriksson and B Johansson *J Alloys and Compounds* **275-277** 472 (1998)

[12] M J Cooper *Rep Prog. Phys.* **48** 415 (1985) and references therein

[13] T Varghese, K M Balakrishna and K Siddappa *Indian J Phys* **76B** 657 (2002)

[14] B L Ahuja and M Sharma *Phys Stat Sol (b)* **241** 2975 (2004)

[15] B L Ahuja, M Sharma and S Mathur *Z Naturf* **59a** 543 (2004), Also B L Ahuja and M Sharma *Solid State Phys.* (India) **46C** (2003) (in Press)

[16] See, for example, D N Timms *Ph D Thesis* (University of Warwick, England)(1989), Also B G Williams Compton Scattering (New York McGraw-Hill) Ch. 3, p 49 (1977)

[17] J Felsteiner, P Pattison and M J Cooper *Phil. Mag* **30** 537 (1974)

[18] F Biggs, L B Mendelsohn and J B Mann *Atomic Data and Nuclear Data Tables* **16** 201 (1975)

[19] K F Berggren *Phys Rev* **B6** 2156 (1972)

[20] B L Ahuja, B K Sharma, and O Aikala *Pramana-J Phys.* **29** 313 (1986)

[21] B K Sharma and B L Ahuja *Phys Rev.* **B38** 3148 (1988)

[22] S Peikkio, B K Sharma, S Manninen, T Paakkari and B L Ahuja *Phys Stat Sol (b)* **168** 657 (1991)

[23] U Mittal, B K Sharma, F M Mohammad and B L Ahuja *Phys Rev* **B38** 12208 (1988)

[24] B L Ahuja, M D Sharma, B K Sharma, S Hamouda and M J Cooper *Phys Scr* **50** 301 (1994)

[25] R K Pandya, K B Joshi, Rajesh Jain, B L Ahuja and B K Sharma *Phys Stat. Sol (b)* **200** 137 (1997)

[26] K B Joshi, Rajesh Jain, R K Pandya, B L Ahuja and B K Sharma *J Chem. Phys* **111** 163 (1999)

[27] C F Fischer *Atomic Data* **4** 301 (1972)

[28] N C Bacalis, N I Papanicolaou and D A Papaconstantopoulos *J. Phys* **F16** 1471 (1986)

[29] N I Papanicolaou, N C Bacalis and D A Papaconstantopoulos *Phys. Rev* **B37** 8627 (1988)

[30] G P Das and P Chaddah *Solid State Commun* **45** 607 (1983)

[31] B L Ahuja and B K Sharma *Phys Lett* **A123** 475 (1987)

[32] M R Norman and D D Koelling *Handbook on the Physics and Chemistry of the Rare Earths* (Amsterdam North-Holland) **Vol 17**, p 1 (1993)

[33] R S Holt and M J Cooper *Phil Mag* **B41** 117 (1980)

[34] L J Nugent, J L Burnett and L R Morss *J Chem. Thermodyn.* **5** 665 (1973)